

Large mechanical squeezing through synthetic magnetism in optomechanics

D. R. Kenigoule Massemblele,^{1,*} P. Djorwé,^{1,2,†} Souvik Agasti,^{3,4,‡} and Amarendra K. Sarma^{5,§}

¹*Department of Physics, Faculty of Science, University of Ngaoundere, P.O. Box 454, Ngaoundere, Cameroon*

²*Stellenbosch Institute for Advanced Study (STIAS), Wallenberg Research Centre at Stellenbosch University, Stellenbosch 7600, South Africa*

³*IMOMEC division, IMEC, Wetenschapspark 1, B-3590 Diepenbeek, Belgium*

⁴*Institute for Materials Research (IMO), Hasselt University, Wetenschapspark 1, B-3590 Diepenbeek, Belgium*

⁵*Department of Physics, Indian Institute of Technology Guwahati, Guwahati 781039, India*

We propose a scheme to generate large amount of mechanical squeezing, far beyond the 3dB limit, which is based on synthetic magnetism in optomechanical system that hosts a Backward Stimulated Brillouin Scattering (BSBS) process. Our benchmark system consists of an acoustic mode coupled to two optical modes through the BSBS process, and a Duffing mechanical oscillator that couples to the same optical modes through the standard optomechanical radiation pressure. The synthetic magnetism comes from the modulation of the mechanical coupling between the acoustic and the mechanical modes. When there is no synthetic magnetism, a given amount of mechanical squeezing is generated in the system. This squeezing is mainly dependent on the BSBS process, and it is fragile against thermal noise. By switching on the synthetic magnetism, the degree of the generated squeezing is greatly enhanced and goes far beyond the limit of the 3dB. This large magnetism induced squeezing persists even when there is no BSBS process in the system. Moreover, this generated squeezing is robust enough against thermal noise in comparison to the one induced when the synthetic magnetism is off. Furthermore, both the mechanical variance squeezing and effective phonon number exhibit series of peaks and dips depending on the phase modulation of the mechanical coupling. This oscillatory feature is reminiscent of a sudden death and revival of squeezing phenomenon, which can be used to maintain a desired magnitude of squeezing by tuning this phase. Our proposal provides a path toward a flexible scheme that generates large amount of squeezing, far beyond the 3dB limit. Such a generated squeezed states can be use for quantum applications including quantum information processing, quantum sensing and metrology, and quantum computing.

Keywords: Optomechanics, synthetic magnetism, squeezing

I. INTRODUCTION

Nonclassical states such as squeezed and entangled states are crucial ingredients required to improve a range of quantum applications including quantum information processing [1–3], quantum sensing/metrology [4–7], quantum computing [8], and quantum supremacy [9–11]. For instance, entangled states have been widely generated in optomechanical systems [12, 13] by exploring diverse techniques [14–18], and they were recently proposed as resources to enhance sensing [19, 20]. Beside that, large intracavity squeezed field have been generated [21, 22], which can be used for mechanical cooling [23, 24], gravitational wave detection [25, 26], and to further generate nonclassical states [27]. Similarly, strong mechanical squeezed states [28] were equally generated, which can be useful to enhance mass-sensing [29–31], phonon information processing [32, 33], and for phononic state transport/transfer [34]. Despite these interesting applications related to squeezed states, their generation is often limited by quantum noise that resists any measurement below the Zero Point Fluctuation (ZPF), i.e., beyond the 3dB limit. The existing systems in which mechanical squeezing beyond 3dB has been achieved have explored reservoir engineering technique or two-tone driving [35–37].

Recently, technique based on synthetic magnetism (engineered via a modulation of the photon/phonon hopping rate) have been used in optomechanical structures for specific purposes. For instance, an artificial magnetic field for photons was engineered to achieve photon transport in [38, 39]. Similarly, synthetic magnetic field for phonon/acoustic has been created in [40–42] for phononic transport at nanoscale. More recently, synthetic magnetism has been engineered in optomechanical systems to enhance entangled states generation [43]. Owing to these interesting physics fostered by synthetic magnetism in optomechanics, here we use it to enhance mechanical squeezing in optomechanical system involving Backward Stimulated Brillouin Scattering (BSBS) process which has been recently proposed [44].

The underlined system consists of an acoustic (mechanical) mode coupled to two optical modes through the BSBS process (radiation pressure coupling). The merit of our proposal is to connect the acoustic and the mechanic modes through a mechanical coupling having a strength J_m that is modulated via a phase θ . Such a phase modulation of the coupling induces a synthetic magnetism in our benchmark system [43, 45]. When the synthetic magnetism is off, a given amount of mechanical squeezing is generated in the system and this squeezing is mainly dependent on the BSBS process, and it is fragile against thermal noise [44]. By switching on the synthetic magnetism, we found that i) the degree of the generated squeezing is greatly enhanced and goes far beyond the limit of the 3dB, ii) this squeezing persists even when there is no BSBS process in the system, and iii) this generated squeezing is robust enough against thermal noise in comparison to the case when the synthetic magnetism is off. Furthermore,

*Electronic address: kenigoule.didier@gmail.com

†Electronic address: djorwepp@gmail.com

‡Electronic address: souvik.agasti@uhasselt.be

§Electronic address: aksarma@iitg.ac.in

both the mechanical squeezing and effective phonon number exhibit series of peaks and dips depending on the phase modulation of the mechanical coupling. This oscillatory feature induces a sudden death and revival of squeezing, which can be used to maintain a desired magnitude of squeezing by tuning this phase. Our proposal pave a way toward a flexible scheme that can be used to generate arbitrary amount of squeezing. Such a generated squeezed states can be used for quantum applications including quantum information processing, quantum sensing and metrology, and quantum computing.

The rest of our work is organized as follow. [section II](#) provides the dynamical equations and derives the analytical expressions involved in our investigation. The squeezing enhancement, together with the important results are presented throughout [section III](#). Our work is concluded in [section IV](#).

II. MODEL AND DYNAMICAL EQUATIONS

Our system consists of an acoustic mode (b_a) that couples to two optical modes through the BSBS process, and a nonlinear mechanical oscillator (b_m) that couples also to the two optical modes. In order to enhance the squeezing of the mechanical oscillator, we assume that the acoustic and mechanical modes are mechanically coupled through a coupling strength J_m , which is modulated through a phase θ that induces a synthetic gauge into the dynamics. The Hamiltonian of such a system is given by ($\hbar = 1$):

$$H = H_0 + H_{OM} + H_{BSBS} + H_{int} + H_{drive}, \quad (1)$$

where

$$H_0 := \sum_{j=1,2} \omega_{c_j} a_j^\dagger a_j + \omega_a b_a^\dagger b_a + \omega_m b_m^\dagger b_m, \quad (2)$$

$$H_{OM} := g_m \sum_{j=1,2} a_j^\dagger a_j (b_m + b_m^\dagger) + \frac{\eta}{2} (b_m + b_m^\dagger)^4, \quad (3)$$

$$H_{BSBS} := -g_a (a_1^\dagger a_2 b_a + a_1 a_2^\dagger b_a^\dagger), \quad (4)$$

$$H_{int} := J_m (e^{i\theta} b_a^\dagger b_m + e^{-i\theta} b_a b_m^\dagger) \quad (5)$$

$$H_{drive} := \sum_{j=1,2} iE_j (a_j^\dagger e^{-i\omega_{p_j} t} - a_j e^{i\omega_{p_j} t}). \quad (6)$$

In the above Hamiltonian, the first term H_0 is the free Hamiltonian of the optical modes a_j , the acoustic and for the mechanical mode. The first term in H_{OM} captures the optomechanical interaction between the optical and the mechanical modes, while the second one accouts for nonlinear effect on the mechanical resonator through the Duffing coefficient η . The third term H_{BSBS} stands for the triply resonant phonon-photon interaction striggered via the BSBS process, and H_{int} depicts the mechanical coupling between the acoustic (b_a) and the mechanical (b_m) modes. The single-photon optomechanical (Brillouin) coupling is captured by g_m (g_a), which comes from the radiation pressure (electrostrictive) force. The drivings fields are captured by the last term H_{drive} , where E_j and ω_{p_j} are the amplitude and frequency of the j^{th} field. In what follow, we will assume the same frequency field,

$\omega_{p1,2} \equiv \omega_p$. The optical cavity frequency are ω_{c_j} and the mechanical (acoustic) frequency is ω_m (ω_a). In the frame rotating at $\frac{\omega_p}{2} a_1^\dagger a_1 + \omega_p a_2^\dagger a_2 + \frac{\omega_p}{2} b_a^\dagger b_a$, the Hamiltonian in [Equation 1](#) becomes

$$H = -\Delta a_1^\dagger a_1 + \Delta_a b_a^\dagger b_a + \omega_m b_m^\dagger b_m - g_m a_1^\dagger a_1 (b_m + b_m^\dagger) + J_m (e^{i\theta} b_a^\dagger b_m + e^{-i\theta} b_a b_m^\dagger) + iE_{l1} (a_1^\dagger - a_1) + \frac{\eta}{2} (b_m + b_m^\dagger)^4 - G_a (a_1^\dagger b_a + a_1 b_a^\dagger), \quad (7)$$

where we have defined $\Delta = \omega_{l1} - \omega_{c1}$, $\Delta_a = \omega_a - \omega_{l1}$ and $G_a = g_a \alpha_2$. Here α_2 is the steady-state of the control optical mode a_2 , which has been treated classically as it is assumed strong compared to the weak strength of the Brillouin acoustic mode b_a .

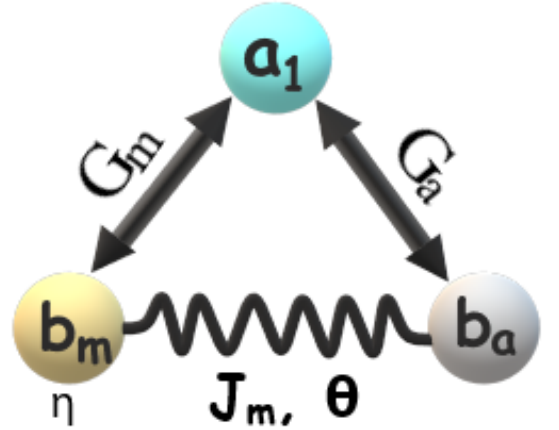


FIG. 1: Sketch of our linearized three mode optomechanical system. The mode a_1 is coupled to the acoustic (mechanical) mode b_a (b_m) the Brillouin (optomechanical) coupling G_a (G_a), which are induced from electrostrictive (radiation pressure) force. The phonon-phonon hopping rate J_m is modulated by the phase θ .

By following the standard linearization process of optomechanical process, the Hamiltonian in [Equation 7](#) can be linearized, and that reduces our proposal to a three modes optomechanical system sketched as in [Figure 1](#). To investigate on the squeezing of the target mechanical resonator b_m , we introduce the following Bogoliubov transformation,

$$b_m = b_m^s \cosh(r) - b_m^{s\dagger} \sinh(r), \quad (8)$$

with the defined squeezing parameter $r = \frac{1}{4} \ln(1 + \frac{2\Lambda}{\omega_m})$ and the squeezed mechanical mode b_m^s . This transformation leads to the new linearized Hamiltonian,

$$H_{lin}^s = -\tilde{\Delta} \delta a_1^\dagger \delta a_1 + \Delta_a \delta b_a^\dagger \delta b_a + \omega'_m \delta b_m^{s\dagger} \delta b_m^s - (G'_m \delta a_1^\dagger + G'_m{}^* \delta a_1) (\delta b_m^{s\dagger} + \delta b_m^s) + J'_m (e^{i\theta} \delta b_a^\dagger \delta b_m^s + e^{-i\theta} \delta b_a \delta b_m^{s\dagger}) - G_a (\delta a_1^\dagger \delta b_a + \delta a_1 \delta b_a^\dagger), \quad (9)$$

with the effective parameters $\omega'_m = \sqrt{\omega_m(\omega_m + 2\Lambda)}$, $G'_m = G_m e^{-r}$ and $J'_m = J_m \cosh(r)$, and the effective mechanical coupling is $G_m = g_m \alpha_1$, where $\Lambda = 24\eta \Re(\beta_m)^2$ by keeping in

mind that β_m (α_1) is the steady-state of the mechanical (optical) mode. By taking into account the optical (κ), mechanical (γ_m) and acoustic (γ_a) dissipations, one can write the dynamics of the fluctuations operators as,

$$\begin{cases} \delta\dot{a}_1 = (\tilde{\Delta} - \frac{\kappa}{2})\delta a_1 + iG'_c(\delta b_m^{s\dagger} + \delta b_m^s) + iG_b\delta b_a \\ \quad + \sqrt{\kappa}a_1^{in} \\ \delta\dot{b}_a = -(\frac{\gamma_a}{2} + i\Delta_a)\delta b_a - iJ'_m e^{i\theta}\delta b_m^s + iG_a\delta a_1 \\ \quad + \sqrt{\gamma_a}b_a^{in} \\ \delta\dot{b}_m^s = -(\frac{\gamma_m}{2} + i\omega'_m)\delta b_m^s - iJ'_m e^{-i\theta}\delta b_a + i(G_m^{*s}\delta a_1 \\ \quad + G'_m\delta a_1^\dagger) + \sqrt{\gamma_m}b_m^{s\dagger}, \end{cases} \quad (10)$$

where $\tilde{\Delta} = \Delta - 2g_m \text{Re}(\beta_m)$ is the effective detuning. In the set of Equation 10, a_1^{in} , b_a^{in} and $b_m^{s\dagger}$ are zero-mean noise operators characterized by the following auto-correlation functions,

$$\begin{aligned} \langle a_1^{in}(t)a_1^{in\dagger}(t') \rangle &= \delta(t-t'), & \langle a_1^{in\dagger}(t)a_1^{in}(t') \rangle &= 0, \\ \langle b_a^{in}(t)b_a^{in\dagger}(t') \rangle &= \delta(t-t'), & \langle b_a^{in\dagger}(t)b_a^{in}(t') \rangle &= 0, \\ \langle b_m^{s\dagger}(t)b_m^{s\dagger}(t') \rangle &= (n_{th} \cosh(2r) + \sinh^2(r))\delta(t-t'), \\ \langle b_m^{in}(t)b_m^{in}(t') \rangle &= (n_{th} + \frac{1}{2})\sinh(2r)\delta(t-t'), \end{aligned} \quad (11)$$

where n_{th} is the equilibrium phonon occupation of the mechanical resonator defined as $n_{th} = [\exp(\frac{\hbar\omega_m}{k_b T}) - 1]^{-1}$, where k_b is the Boltzmann constant. Owing to the high-frequency Brillouin mode b_a compared to the mechanical one ($\omega_m \ll \omega_a$) the thermal acoustic occupancy has been neglected. In order to figure out the effect of the mechanical coupling J_m and its phase modulation θ on the squeezing degree of the targeted mechanical resonator, we start by defined the following amplitude (position) and phase (momentum) quadrature operators, $\delta X_{I,q,a,m} = \frac{\delta\phi^\dagger + \delta\phi}{\sqrt{2}}$, $\delta Y_{\phi,p,a,m} = i\frac{\delta\phi^\dagger - \delta\phi}{\sqrt{2}}$, with $\phi \equiv a_1, b_a, b_m^s$. Similarly, the related noise quadratures read, $\delta X_{I,q,a,m}^{in} = \frac{\delta\phi^{s\dagger in} + \delta\phi^{in}}{\sqrt{2}}$, $\delta Y_{\phi,p,a,m}^{in} = i\frac{\delta\phi^{s\dagger in} - \delta\phi^{in}}{\sqrt{2}}$. Therefore, one derives the set of equations describing the quadrature dynamics of our system as,

$$\dot{u} = Mu + z^{in}, \quad (12)$$

where $u = (\delta I, \delta\phi, \delta q_a, \delta p_a, \delta q_m, \delta p_m)^T$, $z^{in} = (\sqrt{\kappa}I^{in}, \sqrt{\kappa}\phi^{in}, \sqrt{\gamma_a}q_a^{in}, \sqrt{\gamma_a}p_a^{in}, \sqrt{\gamma_m}q_m^{in}, \sqrt{\gamma_m}p_m^{in})^T$ and the matrix M is given by,

$$M = \begin{pmatrix} -\frac{\kappa_1}{2} & -\tilde{\Delta} & 0 & -G_a & 0 & 0 \\ \tilde{\Delta} & -\frac{\kappa_1}{2} & G_a & 0 & 2G'_m & 0 \\ 0 & -G_a & -\frac{\gamma_a}{2} & \Delta'_a & J'_m \sin \theta & J'_m \cos \theta \\ G_a & 0 & -\Delta_a & -\frac{\gamma_a}{2} & -J'_m \cos \theta & J'_m \sin \theta \\ 0 & 0 & -J'_m \sin \theta & J'_m \cos \theta & -\frac{\gamma_m}{2} & \omega'_m \\ 2G'_m & 0 & -J'_m \cos \theta & -J'_m \sin \theta & -\omega'_m & -\frac{\gamma_m}{2} \end{pmatrix}, \quad (13)$$

where the effective couplings G'_m and G_a have been assumed real for simplicity.

III. SYNTHETIC MAGNETISM ENHANCED MECHANICAL SQUEEZING

To point out the enhancement of the mechanical squeezing in our proposed system, we need to derive the position variance of the nonlinear mechanical resonator. For this purpose, we must evaluate the covariance matrix whose elements V_{ij} fulfill $V_{ij} = \frac{\langle u_i u_j + u_j u_i \rangle}{2}$. These matrix elements also satisfy the motional equation,

$$\dot{V} = MV + VM^T + D, \quad (14)$$

with the diagonal diffusion matrix $D = \text{Diag}[\frac{\kappa}{2}, \frac{\kappa}{2}, \frac{\gamma_a}{2}, \frac{\gamma_a}{2}, \frac{\gamma_m}{2}e^{2r}(2n_{th} + 1), \frac{\gamma_m}{2}e^{-2r}(2n_{th} + 1)]$, and the matrix M must meet the Routh-Hurwitz stability criterion where all its eigenvalues should have negative real parts. We have checked that our used parameters satisfy this stability criterion. As we aim to study the steady-state behavior of the mechanical squeezing, we use the long time limit of Equation 14 which is known as Lyapunov equation,

$$MV + VM^T = -D. \quad (15)$$

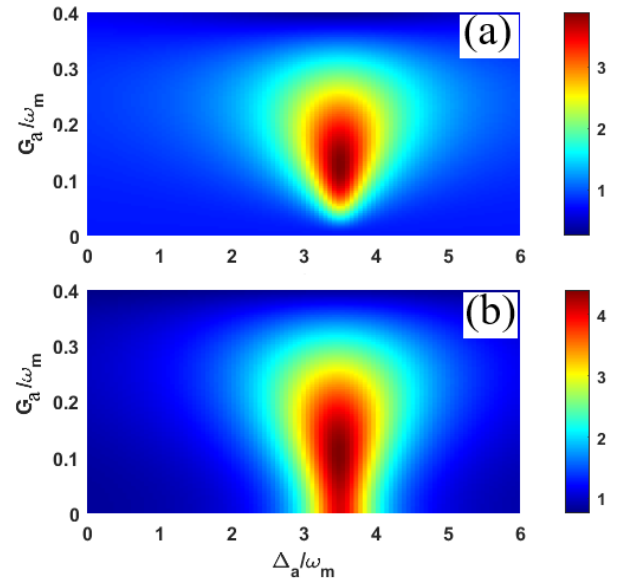


FIG. 2: Mechanical position variance from Equation 17 versus G_a and Δ_a . The mechanical coupling strength is $J_m = 0$ for (a) and $J_m = 0.1\omega_m$ for (b). The parameters used are $\omega_m/2\pi = 1\text{MHz}$, $g_m = 10^{-4}\omega_m$, $\kappa = 0.02\omega_m$, $\gamma_a = 0.4\omega_m$, $\gamma_m = 10^{-4}\omega_m$, $\eta = 10^{-4}\omega_m$, $n_{th} = 100$, $G_m = 0.15\omega_m$, $\tilde{\Delta} = -\omega'_m$, and $\theta = \pi/2$.

From the V_{ij} elements, we can express the position variance ($\langle \delta q_m^2 \rangle$) and the phonon number (n_{eff}^m) of the mechanical resonator as,

$$\langle \delta q_m^2 \rangle = V_{55}e^{-2r}, \quad (16)$$

which can be expressed in dB units as,

$$\langle \delta q_m^2 \rangle (\text{dB}) = -10 \log_{10} \frac{\langle \delta q_m^2 \rangle}{\langle \delta q_{ZPF}^2 \rangle}, \quad (17)$$

where $\langle \delta q_{ZPF}^2 \rangle = \frac{1}{2}$ is the zero-point fluctuations of the mechanical resonator. Before pointing out the effect of the mechanical coupling J_m and its phase θ on the variance squeezing derived in Equation 17, we need to check the optimal acoustic resonance Δ_a^{opt} corresponding to an efficient suppression of the heating term $G'_m(\delta a_1^\dagger \delta b_m^\dagger + \delta a_1 \delta b_m^s)$. For this purpose, we work at the red-sideband detuning ($\tilde{\Delta} = -\omega_m$), and plot the variance by simultaneously sweeping the acoustic effective coupling G_a and detuning Δ_a as shown in Figure 2. It can be seen that the largest squeezing is generated at the acoustic resonance $\Delta_a^{\text{opt}} \approx 3.5\omega_m$ as in [44]. From now on, we fix $\Delta_a = \Delta_a^{\text{opt}}$ from now on, and keep the red-sideband detuning resonance condition. In Figure 2(a), there is no squeezing generated near $G_a \sim 0$, or it is very weak. However, Figure 2(b) shows a large degree of squeezing generated even for $G_a = 0$ around the optimal acoustic resonance Δ_a^{opt} . This feature reveals how the synthetic gauge induces the squeezing in our proposal even if the BSBS effect is not supported in the system. Moreover, the colorbars in these two figures display how the squeezed generated for $J_m \neq 0$ is stronger compared to when there is no mechanical coupling $J_m = 0$. To further get insight into the enhancement of the squeezing through the synthetic gauge, we represent the mechanical position variance together with its effective phonon number, both versus J_m and θ , as displayed in Figure 3. The corresponding mechanical effective phonon number n_{eff}^m can be equally expressed in term of the V_{ij} elements and it yields,

$$n_{eff}^m = \frac{1}{2} (V_{55}e^{-2r} + V_{66}e^{2r} - 1). \quad (18)$$

It can be seen from Figure 3(a,b) that both variance and phonon number are modulated along the θ direction. For $J_m \leq 5 \times 10^{-2}\omega_m$, the effect of the phase θ is not pronounced in these figures. For $J_m > 5 \times 10^{-2}\omega_m$, however, the variance (Figure 3a) exhibits sort of peaks at $\theta \equiv (n + \frac{1}{2})\pi$ and dips for $\theta \equiv n\pi$, with n being an integer. This feature shows that significant squeezing is generated at $\theta \equiv (n + \frac{1}{2})\pi$, which reversely corresponds to an effective minimum phonon number as expected in Figure 3b (see near $J_m \sim 0.1\omega_m$ for instance). By paying attention to the colorbars of these figures, it can be figured out that the more the mechanical coupling J_m increases, the better we cool down the mechanical resonator and that results to a stronger degree of squeezing. These figures point out the crucial role played by both J_m and θ regarding the squeezing enhancement in our proposal. To further reveal the oscillatory feature of the squeezing above discussed, we have extracted the variance and phonon number from Figure 3 at $J_m \sim 0.1\omega_m$, and that is displayed in Appendix A.

In what follow, we aim to figure out the magnitude of the position variance in order to appreciate the degree of the squeezing enhancement induced by the synthetic gauge. By doing so, it can be easy to analyze the behavior of the variance over some parameters instead of just observing its related colorbar as in Figure 2 and Figure 3. Therefore, we pick up specific parameters in the (G_m, G_a) space, and represent the variance over some interesting variables as displayed in Figure 4. The left and right columns in Figure 4 depict the mechanical position variance plotted over the same variable

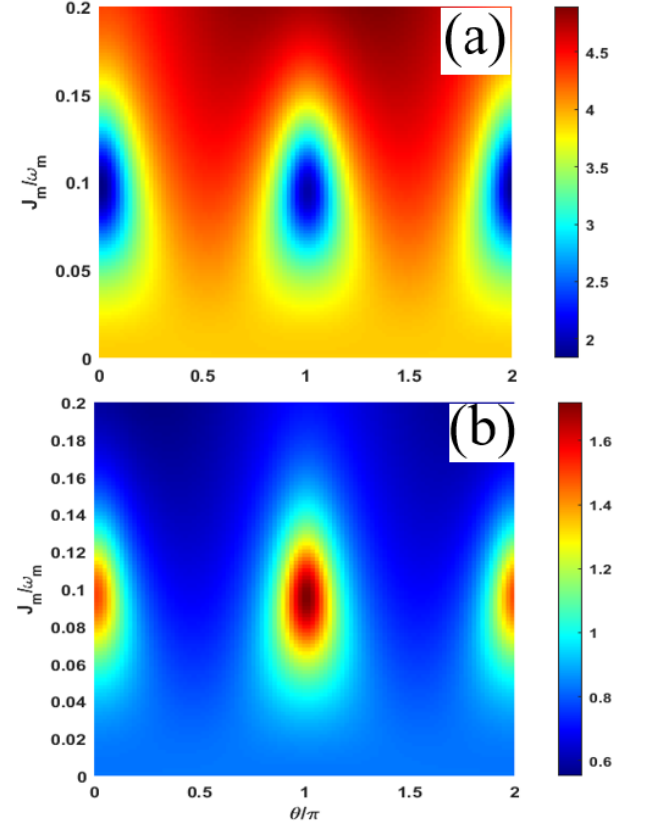


FIG. 3: (a) Mechanical position variance (Equation 17) and (b) mechanical effective phonon number (Equation 18) versus J_m and θ . Optimal squeezing parameters deduced from Figure 2 are used, $G_m = 0.15\omega_m$, $G_a = 0.124\omega_m$, and Δ_a^{opt} . The others parameters are those in Figure 2.

for $J_m = 0$ and $J_m = 0.1\omega_m$, respectively. The first interesting parameter considered here is the Brillouin acoustic decay rate γ_a . The BSBS process involved in our proposal relies on the fact that $\gamma_a \gg \kappa (\gg \gamma_m)$. Therefore, it is crucial to point out the impact of this condition on the squeezing generation as shown in Figure 4(a,b). Without the mechanical coupling ($J_m = 0$), Figure 4a shows how the variance grows up rapidly and reaches a saturation limit above $\gamma_a \gg \kappa = 2 \times 10^{-2}\omega_m$ as expected. Above this BSBS condition, the position variance settles on a sort of plateau, where the acoustic decay rate does no longer affect the behavior of the generated squeezing. This regime could be of great interests for quantum technologies involving squeezing such as quantum information processing, quantum sensing/metrology, and quantum computing. By considering the synthetic gauge ($J_m \neq 0$), Figure 4b shows a great enhancement of the degree of squeezing (from 0 to near 5dB) compared to when $J_m = 0$ (compare Figure 4a to Figure 4b). Despite the fact that the position variance behaves with almost the same shape in both Figure 4(a,b), it is worth to highlight that the merit of the synthetic gauge has been to push the limit of the generated squeezing beyond the 3dB. Furthermore, these figures show that the more the couplings

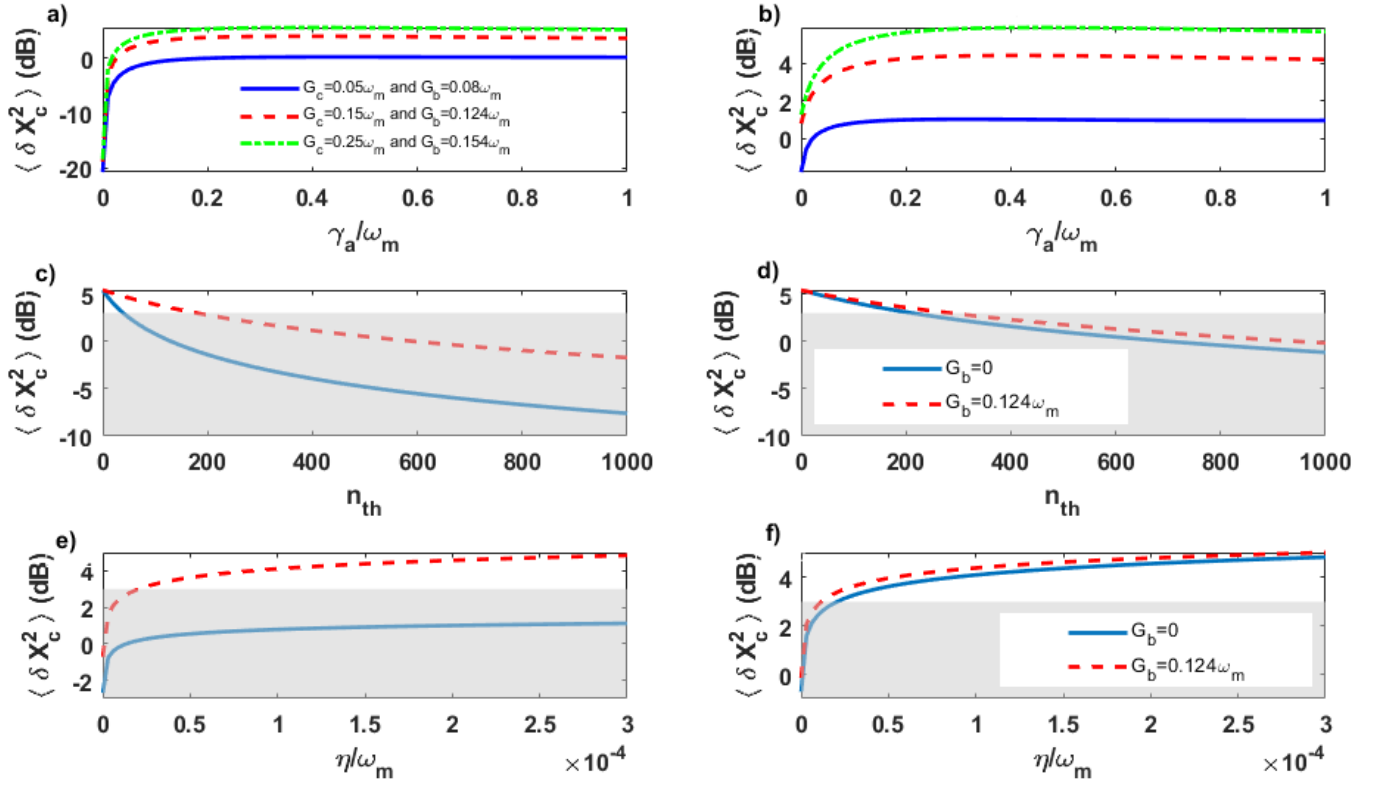


FIG. 4: Left and right column depicts the same quantities, which are plotted for $J_m = 0$ and $J_m = 0.1\omega_m$, respectively. (a,b) display the position variance of the mechanical resonator over the Brillouin acoustic decay rate γ_a for three specific couples of points (G_a, G_m) : $(0.05\omega_m, 0.08\omega_m)$, $(0.15\omega_m, 0.124\omega_m)$, and $(0.25\omega_m, 0.154\omega_m)$. (c,d) analyze the robustness of the mechanical position variance versus the thermal noise n_{th} . (e,f) figure out the behavior of the mechanical position variance versus the Duffing coefficient η . The rest of the parameters are the same as in Figure 2.

(G_m, G_a) are enhanced, better is the degree of the squeezing (see Appendix A for a large view).

In Figure 4c, we have plotted the position variance over the thermal phonon mechanical excitation. The shadow area depicts the region below the 3dB. It can be seen that when $G_a = 0$, there is only a short window where the squeezing is above the 3dB (full line) compared to when $G_a \neq 0$ (dashed line). This feature reveals the key role played by the BSBS effect, which suppresses heating processes in the system [44]. This BSBS effect is further reinforced through the gap between the two lines in Figure 4c, showing how $G_a \neq 0$ has improved the degree of squeezing compared to the case $G_a = 0$. By taking into account the synthetic gauge, the first observation in Figure 4d is the gap between the cases $G_a = 0$ and $G_a \neq 0$ that has been efficiently reduced. Indeed, the squeezing generated for $G_a = 0$ follows almost the one generated for $G_a \neq 0$, and they stay longer beyond the 3dB compared to what is shown in Figure 4d. This confirms that the synthetic gauge contributes to suppress heating channels, inducing strong squeezing even for $G_a = 0$, as earlier discussed in Figure 2. Furthermore, it can be observed that the squeezing resists more to the mechanical thermal noise when the synthetic gauge is accounted. In Figure 4(e,f), we display the mechanical position variance versus the Duffing nonlinear coefficient

η . These figures show how the variance sharply grows for weak values of η , and settles quickly to a plateau like a saturation limit. However, it can be observed that the synthetic gauge bridges the gap between the cases $G_a = 0$ and $G_a \neq 0$ as previously discussed. Moreover, Figure 4e shows how the degree of the generated squeezing for $G_a = 0$ is below the 3dB, while it exceeds this limit for $J_m \neq 0$ as depicted in Figure 4f. Once again, this reveals the merit of the synthetic gauge that induces a strong squeezing even for $G_a = 0$ in our proposal as shown in Figure 2.

In order to have a concise representation of these squeezed states generated in our proposal, we move to the phase space where we provide Wigner function distribution for specific parameters. Owing to the Gaussian nature of the quantum noise, our linearized system can be captured through a single Gaussian Wigner function in the steady state defined as [28]

$$W(u_m) = \frac{1}{2\pi\sqrt{\det[V_m]}} \exp\left[-\frac{u_m^T V_m^{-1} u_m}{2}\right], \quad (19)$$

where $u_m = (\delta q_m, \delta p_m)^T$ is the column vector of the mechanical fluctuations and V_m stands for the covariance matrix for the mechanical mode. The left column in Figure 5 depicts the Wigner function distribution of the mechanical resonator

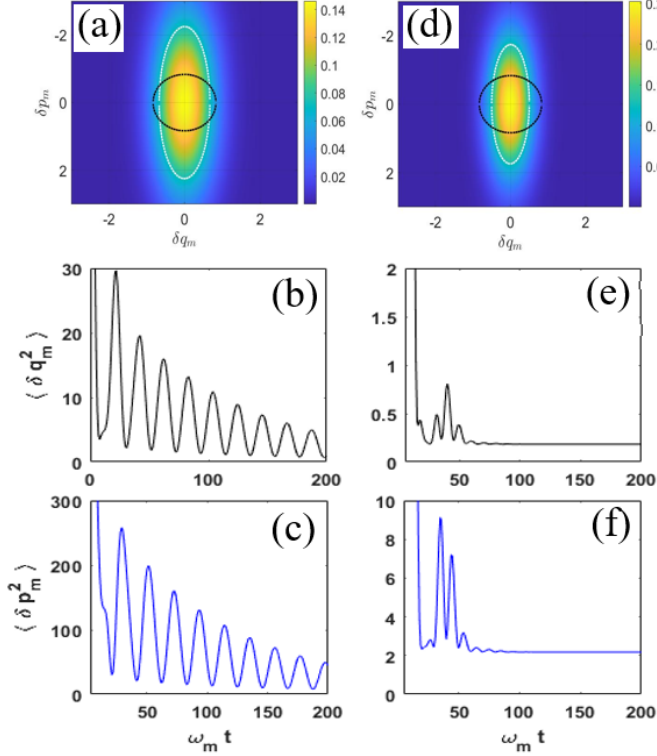


FIG. 5: Wigner function distributions and dynamic of mechanical variances. Left column depicts Wigner function (a), position variance (b) and the momentum variance (c) at $J_m = 0.1\omega_m$, and $\theta = 0$. Right column depicts Wigner function (d), position variance (e) and the momentum variance (f) at $J_m = 0.1\omega_m$, and $\theta = \pi/2$. These figures are extracted from the feature displayed in Figure 3. The other parameters are the same as in Figure 2.

(Figure 5a), the mechanical position variance (Figure 5b) and the mechanical momentum variance (Figure 5c) for the synthetic modulation phase of $\theta = 0$. Similarly, the right column displays the same quantities at $\theta = \frac{\pi}{2}$ i.e., the Wigner function distribution (Figure 5d), the position variance (Figure 5e) and the momentum variance (Figure 5f). These figures have been captured for a long time enough that the system has reached its steady state dynamic. Moreover, these figures have been extracted from Figure 3a for the mechanical coupling strength fixed at $J_m = 0.1\omega_m$. In Figure 5(a,d), the contour represented by a dark circle depicts the related coherent state, while the shrunken and expanded shape bounded by the white ellipsis features the corresponding generated squeezed state. As predicted from Figure 3a, the wigner function at $\theta = 0$ (Figure 5a) shows less squeezing as compared to when $\theta = \pi/2$ (Figure 5d). Moreover, these Wigner function distributions confirm the squeezing along the position direction, while the quantum fluctuation is transferred to the momentum direction which is amplified. To further analyze these observations, we have plotted the dynamical time-evolution of the involved variances. As expected, both position and momentum dynamical evolution at $\theta = 0$ clearly show no squeezing (Figure 5(b,c)), which is revealed by an oscillatory behavior

above the Standard Quantum Limit (SQL). However, we can qualitatively observe that there is less amount of noise along the position direction compared to the momentum direction as predicted by the corresponding Wigner distribution (Figure 5a). For $\theta = \pi/2$, however, Figure 5e shows squeezing degree below the SQL, while its corresponding momentum is far above the SQL, revealing that quantum fluctuation has been amplified along this direction as predicted from Figure 5d. From the above analysis, it can be seen that our Wigner function distribution together with the dynamical evolution of the variances agree well with the synthetic magnetism squeezing enhancement pointed out in Figure 3. This work provides an efficient scheme toward squeezing enhancement beyond 3dB in optomechanical system that is based on backward stimulated Brillouin scattering effect. The generated squeezing under this scheme is robust enough against thermal noise compared to the case without the synthetic magnetism. This investigation can be extended to electromechanical systems, hybrid opto-electromechanical system and to connexe fields.

IV. CONCLUSION

We have investigated on a synthetic magnetism effect inducing mechanical squeezing enhancement in an optomechanical system, which hosts a backward stimulated Brillouin scattering process. Our benchmark system consists of an acoustic mode that couples to two optical modes through the BSBS process, and a nonlinear mechanical oscillator that couples to the two optical modes through the standard optomechanical radiation pressure. A mechanical coupling, with a strength J_m that is modulated through a phase θ , is connecting the acoustic and mechanical modes, which induces a synthetic magnetism in our proposal. Without this synthetic magnetism, there is a given amount of squeezing that is generated in the system. This squeezing is mainly induced by the BSBS process, and is fragile against thermal noise. When the synthetic magnetism is accounted, the degree of the generated squeezing is greatly enhanced and goes far beyond the 3dB. Moreover, this large induced squeezing persists even when the system is free from the BSBS process. Furthermore, this generated squeezing is robust enough against thermal noise compared to the case without synthetic magnetism. Another merit of the synthetic magnetism in our proposal is revealed through the peaks and dips of both squeezing magnitude and mechanical effective phonon number depending on the modulation phase of the mechanical coupling. This oscillatory feature is reminiscent of a sudden death and revival of squeezing phenomenon, which can be used to maintain a desired magnitude of squeezing by tuning the phase θ . Our work sheds light on a flexible scheme that can be used to generate a large amount of mechanical squeezing, far beyond the 3dB limit. Our scheme can be implemented in optical and microwaves cavities, as well as in hybrid optomechanical systems. Such a generated squeezed states can be useful for range of quantum applications including quantum information processing, quantum sensing/metrology, and the recent development in quantum computing.

Acknowledgments

Funding: This work has been carried out under the Iso-Lomso Fellowship at Stellenbosch Institute for Advanced Study (STIAS), Wallenberg Research Centre at Stellenbosch University, Stellenbosch 7600, South Africa. P. Djorwe acknowledges the receipt of a grant from the APS-EPS-FECS-ICTP Travel Award Fellowship Programme (ATAP), Trieste, Italy. S. Agasti wishes to acknowledge the European Union; Project number: 101065991 (acronym: SingletSQL) for sup-

porting the work. A.K. Sarma acknowledges the STARS scheme, MoE, government of India (Proposal ID 2023-0161).

Appendix A: Linearization

Appendix B: Bogoliubov transformation

-
- [1] G. Wendin, Reports on Progress in Physics **80**, 106001 (2017), ISSN 1361-6633.
 - [2] S. Slussarenko and G. J. Pryde, Applied Physics Reviews **6**, 041303 (2019), ISSN 1931-9401.
 - [3] N. Meher and S. Sivakumar, The European Physical Journal Plus **137**, 985 (2022), ISSN 2190-5444.
 - [4] C. Degen, F. Reinhard, and P. Cappellaro, Reviews of Modern Physics **89** (2017), ISSN 1539-0756.
 - [5] E. Polino, M. Valeri, N. Spagnolo, and F. Sciarrino, AVS Quantum Science **2**, 024703 (2020).
 - [6] B. Stray, A. Lamb, A. Kaushik, J. Vovrosh, A. Rodgers, J. Winch, F. Hayati, D. Boddice, A. Stabrawa, A. Niggebaum, et al., Nature **602**, 590 (2022), ISSN 1476-4687.
 - [7] M. Barbieri, PRX Quantum **3**, 010202 (2022).
 - [8] M. Zidan, H. Eleuch, and M. Abdel-Aty, Results in Physics **21**, 103536 (2021), ISSN 2211-3797.
 - [9] F. Arute, K. Arya, R. Babbush, D. Bacon, J. C. Bardin, R. Barends, R. Biswas, S. Boixo, F. G. S. L. Brandao, D. A. Buell, et al., Nature **574**, 505 (2019), ISSN 1476-4687.
 - [10] H.-S. Zhong, H. Wang, Y.-H. Deng, M.-C. Chen, L.-C. Peng, Y.-H. Luo, J. Qin, D. Wu, X. Ding, Y. Hu, et al., Science **370**, 1460 (2020), ISSN 1095-9203.
 - [11] H.-S. Zhong, Y.-H. Deng, J. Qin, H. Wang, M.-C. Chen, L.-C. Peng, Y.-H. Luo, D. Wu, S.-Q. Gong, H. Su, et al., Physical Review Letters **127** (2021), ISSN 1079-7114.
 - [12] M. Aspelmeyer, T. J. Kippenberg, and F. Marquardt, Reviews of Modern Physics **86**, 1391 (2014), ISSN 1539-0756.
 - [13] D. P. Foulia, P. Djorwé, S. T. Kingni, and S. G. N. Engo, Physical Review A **95**, 123 (2017).
 - [14] R. Riedinger, A. Wallucks, I. Marinković, C. Löschner, M. Aspelmeyer, S. Hong, and S. Gröblacher, Nature **556**, 473 (2018), ISSN 1476-4687.
 - [15] C. Tchodimou, P. Djorwe, and S. G. N. Engo, Physical Review A **96** (2017).
 - [16] S. Kotler, G. A. Peterson, E. Shojaei, F. Lecocq, K. Cicak, A. Kwiatkowski, S. Geller, S. Glancy, E. Knill, R. W. Simmonds, et al., Science **372**, 622 (2021), ISSN 1095-9203.
 - [17] S. Chakraborty and A. K. Sarma, Physical Review A **100**, 063846 (2019), ISSN 2469-9934.
 - [18] D. R. K. Massembele, P. Djorwé, A. K. Sarma, and S. G. N. Engo, arXiv (2024).
 - [19] Y. Xia, A. R. Agrawal, C. M. Pluchar, A. J. Brady, Z. Liu, Q. Zhuang, D. J. Wilson, and Z. Zhang, Nature Photonics **17**, 470 (2023), ISSN 1749-4893.
 - [20] A. J. Brady, X. Chen, Y. Xia, J. Manley, M. Dey Chowdhury, K. Xiao, Z. Liu, R. Harnik, D. J. Wilson, Z. Zhang, et al., Communications Physics **6** (2023), ISSN 2399-3650.
 - [21] H. Vahlbruch, M. Mehmet, K. Danzmann, and R. Schnabel, Physical Review Letters **117** (2016), ISSN 1079-7114.
 - [22] W. Qin, A. Miranowicz, and F. Nori, Physical Review Letters **129** (2022), ISSN 1079-7114.
 - [23] J. B. Clark, F. Lecocq, R. W. Simmonds, J. Aumentado, and J. D. Teufel, Nature **541**, 191 (2017), ISSN 1476-4687.
 - [24] P. Djorwé, J. H. T. Mbé, S. G. N. Engo, and P. Wofo, Physical Review A **86**, 043816 (2012).
 - [25] J. Aasi, J. Abadie, B. P. Abbott, R. Abbott, T. D. Abbott, M. R. Abernathy, C. Adams, T. Adams, P. Addesso, R. X. Adhikari, et al., Nature Photonics **7**, 613 (2013), ISSN 1749-4893.
 - [26] B. P. A. et al., Physical Review Letters **116**, 061102 (2016).
 - [27] W. Qin, A. Miranowicz, H. Jing, and F. Nori, Physical Review Letters **127** (2021), ISSN 1079-7114.
 - [28] P. Banerjee, S. Kalita, and A. K. Sarma, Journal of the Optical Society of America B **40**, 1398 (2023), ISSN 1520-8540.
 - [29] P. Djorwe, Y. Pennec, and B. Djafari-Rouhani, Physical Review Applied **12**, 024002 (2019).
 - [30] S. M. Tchounda, P. Djorwé, S. N. Engo, and B. Djafari-Rouhani, Physical Review Applied **19**, 064016 (2023), ISSN 2331-7019.
 - [31] P. Djorwé, M. Asjad, Y. Pennec, D. Dutykh, and B. Djafari-Rouhani, arXiv (2023).
 - [32] K. Stannigel, P. Komar, S. J. M. Habraken, S. D. Bennett, M. D. Lukin, P. Zoller, and P. Rabl, Physical Review Letters **109** (2012), ISSN 1079-7114.
 - [33] G. Madiot, R. C. Ng, G. Arregui, O. Florez, M. Albrechtsen, S. Stobbe, P. D. García, and C. M. Sotomayor-Torres, Physical Review Letters **130** (2023), ISSN 1079-7114.
 - [34] H. Ren, T. Shah, H. Pfeifer, C. Brendel, V. Peano, F. Marquardt, and O. Painter, Nature Communications **13** (2022), ISSN 2041-1723.
 - [35] M. J. Woolley and A. A. Clerk, Physical Review A **89** (2014), ISSN 1094-1622.
 - [36] E. E. Wollman, C. U. Lei, A. J. Weinstein, J. Suh, A. Kronwald, F. Marquardt, A. A. Clerk, and K. C. Schwab, Science **349**, 952 (2015), ISSN 1095-9203.
 - [37] C. Lei, A. Weinstein, J. Suh, E. Wollman, A. Kronwald, F. Marquardt, A. Clerk, and K. Schwab, Physical Review Letters **117** (2016), ISSN 1079-7114.
 - [38] M. Schmidt, S. Kessler, V. Peano, O. Painter, and F. Marquardt, Optica **2**, 635 (2015).
 - [39] K. Fang, Z. Yu, and S. Fan, Nature Photonics **6**, 782 (2012).
 - [40] C. Brendel, V. Peano, O. J. Painter, and F. Marquardt, Proceedings of the National Academy of Sciences **114** (2017).
 - [41] J. P. Mathew, J. del Pino, and E. Verhagen, Nature Nanotechnology **15**, 198 (2020).
 - [42] X. Wang, H.-R. Li, and F.-L. Li, New Journal of Physics **22**, 033037 (2020).

- [43] D.-G. Lai, J.-Q. Liao, A. Miranowicz, and F. Nori, *Physical Review Letters* **129**, 063602 (2022).
- [44] S.-S. Chen, N.-N. Zhang, Y.-R. Guo, H. Yang, and Y. Ma, *arXiv* (2023).
- [45] P. Djorwé, H. Alphonse, S. Abbagari, S. Doka, and S. N. Engo, *Chaos, Solitons and Fractals* **170**, 113333 (2023), ISSN 0960-0779.